# Nonuniversal critical behavior of magnetic dipoles on a square lattice

Julio F. Fernández[1,*] and Juan J. Alonso[2,†]
[1]*ICMA, CSIC and Universidad de Zaragoza, 50009-Zaragoza, Spain*
[2]*Física Aplicada I, Universidad de Málaga, 29071-Málaga, Spain*
(Received 20 February 2007; revised manuscript received 29 May 2007; published 3 July 2007)

We study the thermal transition between the paramagnetic and antiferromagnetic phases of interacting magnetic dipoles on square lattices in two dimensions. By Monte Carlo simulations, we find strong long-range order in the low temperature phase and a critical behavior that is, as in the fourfold anisotropic *XY* model, nonuniversal, in that the single-site quadrupolar anisotropy $h_4$ is a relevant variable. However, the critical indices differ markedly from the ones for the anisotropic *XY* model. They vary from Ising type, within errors, for $h_4=0$, to a critical behavior in the $h_4\to\infty$ limit that is nearly as abrupt as a first-order transition.

DOI: 10.1103/PhysRevB.76.014403 PACS number(s): 75.10.−b, 75.40.Cx, 75.40.Mg

## I. INTRODUCTION

There is currently renewed interest in systems of classical dipoles (SCD's). Some of the interest comes from the emerging field of nanoscience.[1] Arrays of magnetic nanoparticles[2] and of synthesized crystals of organometallic molecules,[3] in which dipole-dipole interactions play an important role, are becoming available for experiment. In addition, SCD's are intrinsically interesting. The spatial variations of the magnetic field from each of the dipoles in the system give rise to interesting anisotropy effects as well as frustration (i.e., the outcome from interactions which cannot all be concurrently satisfied). Frustration makes SCD's highly sensitive to spatial arrangement. Different magnetically ordered states ensue in different lattices,[4] including "spin ice" in some exotic lattices.[5] In two dimensions (2D), anisotropy plays an important role in ordering SCD's. Single site anisotropy is always present in magnetic-crystalline systems, but dipole-dipole interactions give rise to two further types of anisotropies in SCD's in 2D. The first one pushes spins to lie on the plane of the lattice.[6] One therefore expects dipolar *XY* (*dXY*) models, that is, systems of planar spins with dipole-dipole interactions, to be relevant to the critical behavior of SCD's on a 2D lattice. The second anisotropy arises from dipolar interactions in a different manner. The ground state itself is invariant under a continuous staggered rotation (SR) of all spins,[7–9] such as the one that takes the spin configuration in Fig. 1(a) into the one shown in Fig. 1(b). On the other hand, the Hamiltonian itself varies under any continuous rotation, but is clearly invariant under fourfold homogeneous rotation of all spins *and* of all site positions, such as the one that takes Fig. 1(b) into Fig. 1(c). Thus, continuous SR invariance is not expected to survive thermal disorder, only fourfold SR invariance is expected to do so. Indeed, Prakash and Henley[10] showed how thermal excitations in a model of *XY* spins on a square lattice, with a nearest-neighbor version of dipole-dipole interactions, lead to effective anisotropies, an effect which they termed "ordering due to disorder."[10] It has been subsequently explored in some detail by various means.[9,11]

In order to illustrate the quadrupolar anisotropy effect that ensues, as first derived in Ref. 10, from thermal effects in SCD's on square lattices, let us define

$$\mathfrak{m}_x = N^{-1}\sum_i \tau_i^x S_i^x, \tag{1}$$

and similarly for $\mathfrak{m}_y$, where

$$\tau_x = (-1)^{ky}, \quad \tau_y = (-1)^{kx}, \tag{2}$$

and $k_x$ and $k_y$ are the $x$ and $y$ component site numbers, respectively. Plots of various probability densities for the order parameter $(\mathfrak{m}_x, \mathfrak{m}_y)$ to point in different directions are shown in Fig. 1(d). A similar plot for a nearest-neighbor *XY* or Heisenberg model would give $f(\theta)$ independent of $\theta$. For comparison, we have added a quadrupolar anisotropy,

$$\mathcal{H}_A = -h_4\sum_i [(S_i^x)^4 + (S_i^y)^4], \tag{3}$$

to the Heisenberg model, and performed on it a Monte Carlo (MC) simulation at $k_bT=0.3J$ with $h_4=0.06J$. Results for various system sizes are plotted in Fig. 1(e). Note the similarity, even in the size dependence of $f(\theta)$. There is no similarity, however, in their $T$ dependence: whereas $f(\theta)$ is approximately independent of $T$ in the Heisenberg model, it vanishes as $T\to 0$ in SCD's.[9]

Anisotropy has a deeper effect on the ordering of SCD's in 2D than the range of dipolar interactions. An *isotropic* caricature of dipole-dipole interactions seems not to lead to *strong* long-range order in square lattices,[13] only to *weak* long-range order[14] at low temperatures. (This is so in spite of the fact that the theorem of Mermin and Wagner[12] does not rule out strong long-range order in SCD's in 2D.) On the other hand, true dipole-dipole interactions, do lead to strong long-range order.[15,16] Results from MC simulations also suggest strong order in SCD's in 2D at low temperatures.[9,11] This suggests that the thermal anisotropy induced by dipole-dipole interactions[10] is relevant to the critical behavior of SCD's. This would be as in the standard *XY* model, in which anisotropies also lead to strong long-range order.[17]

It is our aim to study by MC simulations the critical properties of SCD's on square lattices, whether they fit into some universality class, independently of the strength, $h_4$, of quadrupolar interactions, or whether nonuniversal critical behavior ensues, as it does in *XY* models with a fourfold anisotropy.[17]

 

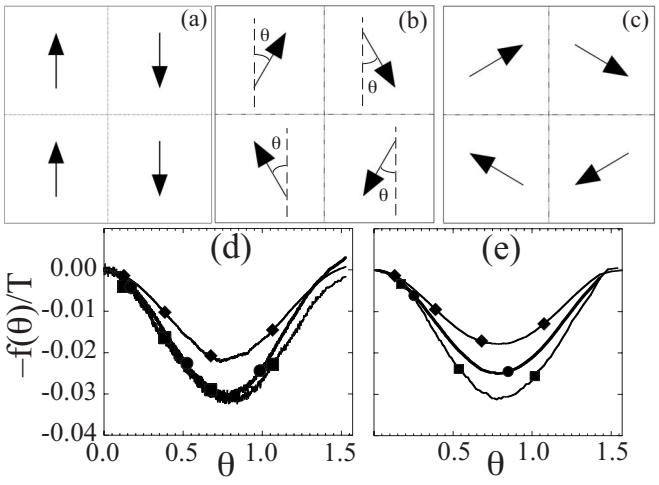


FIG. 1. (a) Collinear state. (b) Canted state, which follows from the collinear state in (a) by performing a staggered rotation by angle $\theta$. (c) State obtained by a $\pi/2$ rotation of both the lattice *and* of all spins. (d) Free energy per spin over temperature, $T$, versus the order parameter orientation angle $\theta$ of the SCD's at $k_BT=0.25\varepsilon_d$ for systems of $L\times L$ spins. ■, ●, and ◆ stand for $L=4,8$, and 16. The data were extracted from runs of some $5\times10^7$ MC sweeps, during which the angle $\theta$ of the order parameter $(\mathfrak{m}_x,\mathfrak{m}_y)$ is monitored. We obtain $f(\theta)$ from the number of recorded events $n(\theta)$ for angle $\theta$, defined by $\arctan(\mathfrak{m}_y/\mathfrak{m}_x)$, in some small ($\sim$0.0015) interval, using the expression $n(\theta)\propto\exp[-Nf(\theta)]$. (e) Same as in (d) but for a classical nearest-neighbor Heisenberg model on a square lattice at $k_BT=0.3|J|$, with an anisotropy energy $h_4\Sigma_i[(S_i^x)^4+(S_i^y)^4]$ and $h_4=0.06|J|$.

The plan of the paper is as follows. The model (SCD's on square lattices), boundary (periodic) conditions, and details about our MC simulations are specified in Sec. II. There is no exchange, only dipole-dipole interactions and a single-site quadrupolar anisotropy. In Sec. III, we report results for three values $(0,4,\infty)$ of $h_4$. For $h_4=\infty$, we simulate a dipolar four-state clock model (D4CM), that is, a system of two component spins which can point in four evenly spaced directions, as in the well-known four-state clock model,[17] but interact among themselves through magnetic dipolar fields. We find a single transition between paramagnetic and fully ordered phases for all three values of $h_4$. As in the anisotropic $XY$ model,[17] nonuniversal critical behavior as a function of the quadrupolar anisotropy strength is found. On the other hand, our numerical results (given in Table I) differ sharply from the ones for the anisotropic $XY$ model. Finally, we summarize and discuss our results in Sec. IV.

## II. MODEL AND CALCULATION

We first define the SCD. Let $\mathbf{S}_i$ be a classical three-component unit spin at lattice site $i$ of a two-dimensional square lattice, let

$$\mathcal{H}=\mathcal{H}_d+\mathcal{H}_A, \tag{4}$$

where

$$\mathcal{H}_d=\sum_{\langle ij\rangle}\sum_{\alpha\beta}T_{ij}^{\alpha\beta}S_i^\alpha S_j^\beta, \tag{5}$$

TABLE I. Variation of the critical indices with quadrupolar anisotropy.

| $h_4$ | $T_c$ | $\beta/\nu$ | $\eta$ | $\alpha/\nu$ | $\nu$ |
|---|---|---|---|---|---|
| 0 | 0.580(5) | 0.13(2) | 0.23(2) | $\lesssim$0.1 | 1.05(5) |
| 4 | 0.857(2) | 0.10(1) | 0.20(4) | 0.51(4) | 0.74(5) |
| $\infty$ | 1.106(2) | 0.03(2) | 0.09(5) | 0.82(5) | 0.70(5) |

$$T_{ij}^{\alpha\beta}=\varepsilon_d\left(\frac{a}{r_{ij}}\right)^3\left(\delta_{\alpha\beta}-3\frac{r_{ij}^\alpha r_{ij}^\beta}{r_{ij}^2}\right), \tag{6}$$

$\mathbf{r}_{ij}$ is the displacement from site $i$ to site $j$, $a$ is the SC lattice parameter. The nearest-neighbor dipolar energy $\varepsilon_d$ is defined through Eqs. (5) and (6). We give all energies in terms of $\varepsilon_d$.

In the D4CM, everything is as for SCD's except that spins can only point along any of the four directions of the square lattice, as if $h_4\to\infty$ in SCD's.

We use periodic boundary conditions (PBC's), which, for the sake of simplicity, we explain for one dimension. Consider first spin sites at $x_k=ka$, for $k=-\infty\cdots-1,0,1\cdots\infty$. $S_k^\alpha=S_{k+L}^\alpha$ for all $k$, and we let a spin at the $k$th site interact with all $L/2$ $(L/2-1)$ spins immediately to the right-hand (left-hand) side of the $k$th site.

Our simulations follow the standard Metropolis MC algorithm.[18] In particular, after we choose an initial spin configuration, we compute the dipolar field at each site. Time evolution takes place as follows. A spin is chosen at random and temporarily pointed in a new random direction. The move is accepted if either $\Delta E\leq0$, where $\Delta E$ is the energy change, or with probability $\exp(-\Delta E/k_BT)$ if $\Delta E>0$. All dipolar fields are then updated throughout the system if the move is accepted, before another spin is chosen to repeat the process.

All energies and temperatures are given in terms of $\varepsilon_d$ and $\varepsilon_d/k_B$, respectively.

Unless we state otherwise, all numerical results may be assumed to come from averages over some $10^7$ MC sweeps, having first disregarded near $10^5$ MC sweeps. Within the temperature range we cover, the results thus obtained seem independent of the initial conditions, that is, of whether the initial state is ordered, disordered or is the outcome of some previous cooling process.

For easy reference, we next define the quantities we calculate. We let

$$\phi=\left\langle\sqrt{\mathfrak{m}_x^2+\mathfrak{m}_y^2}\right\rangle, \tag{7}$$

where $\mathfrak{m}_x$ and $\mathfrak{m}_y$ are defined in Eqs. (1) and (2), and

$$\mathcal{S}=N\langle\mathfrak{m}_x^2+\mathfrak{m}_y^2\rangle. \tag{8}$$

We obtain the specific heat $C$ from the energy fluctuations relation $C=\delta E^2/(Nk_BT^2)$, where $\delta E$ is the root-mean-square average of the system energy over some MC run at temperature $T$.

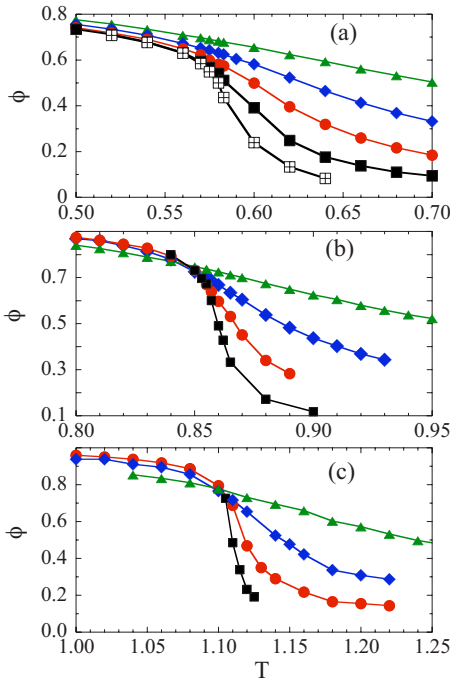


FIG. 2. (Color online) (a) $\phi$ vs $T$ for SCD's with $h_4=0$. ▲, ◆, ●, ■, and ⊞ stand for $L=8,16,32,64$, and 128, respectively. Lines are only guides for the eyes. (b) Same as in (a) but for $h_4=4$. (c) Same as in (a) but for $h_4=\infty$.

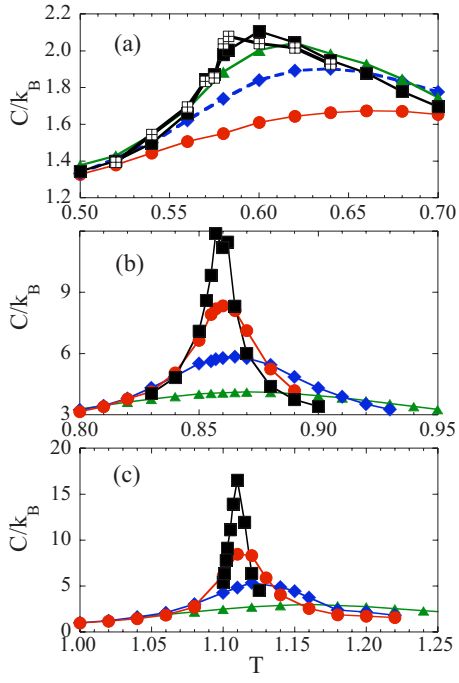


FIG. 3. (Color online) (a) Specific heat vs $T$ for SCD's with $h_4=0$. ▲, ◆, ●, ■, and ⊞ stand for $L=8,16,32,64$, and 128, respectively. Lines are only guides for the eyes. (b) Same as in (a) but only for $L\leq 64$, for SCD's with $h_4=4$. (c) Same as in (b) but for $h_4=\infty$.

## III. RESULTS

In this section we report MC data obtained for SCD's with $h_4=0$, 4, and $\infty$, and obtain the critical index values which we give in Table I.

The data obtained for the order parameter $\phi$ are plotted vs $T$ in Figs. 2(a), 2(b), and 2(c), for $h_4=0,4$, and $\infty$, respectively. Clearly, a disordered phase can be inferred for $T \gtrsim 0.58$ from Fig. 2(a). At lower temperatures, *strong* long-range order is not immediately obvious. In the $0.5 \lesssim T \lesssim 0.58$ range, $\phi$ appears to decrease slowly as $L$ increases, at least up to $L=64$. We return to this point in the discussion of Fig. 4, which follows below. Further information is provided in the plots of the specific heat vs $T$, in Figs. 3(a), 3(b), and 3(c), for $h_4=0,4$, and $\infty$, respectively. We note from Figs. 2(b) and 2(c) that $\phi$ drops to zero more steeply as $h_4$ increases. Strengthening of the specific heat singularity as $h_4$ increases is also clear. However, we draw no quantitative results from these plots.

We first examine whether weak long-range order exists in SCD's for $h_4 \geq 0$. For that purpose, we examine log-log plots of $\phi$ vs $L$. They are shown in Figs. 4(a), 4(b), and 4(c) for $h_4=0,4$, and $\infty$, respectively. In the $0.52 \lesssim T \lesssim 0.58$ range of Fig. 4(a), there appears to be a crossover from $\phi \propto L^{-\beta/\nu}$, with $\beta>0$ in the $8 \leq L \leq 64$ range, to a $\phi$ that is approximately independent of $L$ in the $64 \leq L \leq 128$ range. This is why we took the trouble to run large time consuming simulations for $L=128$ systems. Without the data points for $L=128$, one would have been tempted to infer the existence of an intermediate phase, in the $0.52 \lesssim T \lesssim 0.58$ range, of weak long-range order. Information about the nature of a transition can also be gathered from the fourth-order cumulantlike quantity $u=1-\langle\phi^4\rangle/3\langle\phi^2\rangle^2$.[19] In plots of $u$ vs $T$ for $L=64$ and $L=128$ (not shown), the two curves increase smoothly and monotonically as $T$ decreases. Quantity $u$ is larger for $L=128$ ($L=64$) at low (high) temperature. The two curves cross at $T \simeq 0.575$, $u \simeq 0.66$. The data for $u$ show no trace of anything but of a standard second-order transition. For $h_4=0$, we thus infer the existence of a single thermal transition, at $T_c \simeq 0.58$, between the paramagnetic and fully ordered antiferromagnetic phases. This is in contrast to the reported behavior of an intermediate phase[20] in the ordinary $XY$ model with weak anisotropy. Because there is a thermally induced anisotropy in SCD's in 2D,[10] the comparison is appropriate, even though $h_4=0$. Note, however, that the thermally induced anisotropy in SCD's in square lattices is not too weak. For further remarks on this point, see Sec. IV. For $h_4=4$ and $h_4=\infty$ strong long-range order below $T_c$ is consistent with the plots in Figs. 4(b) and 4(c). Log-log plots of $\mathcal{S}$ vs $L$, for $h_4=4$ and $\infty$, are shown in Figs. 5(b) and 5(c), respectively, for various temperatures. Again, we see no intermediate phase. Furthermore, strong long-range order seems to follow, as it does from Figs. 4(b) and 4(c), for temperatures below the values of $T_c$ given in Table I.

For the critical behavior, we make use of finite size scaling,[21]

$$\phi \sim L^{-\beta/\nu} f_1(\xi/L), \tag{9}$$

where $\xi$ is the spin-spin correlation length, $\beta$ and $\nu$ are the usual critical indices,[22] defined by $\phi \sim (T_c - T)^\beta$ and $\xi \sim |T_c - T|^\nu$ that hold for an infinite system, and $f_1(x)$ is some function of $x$. Similarly, $\mathcal{S} \sim L^{d-\eta} f_2(\xi/L)$ and $C \sim L^{\alpha/\nu} f_3(\xi/L)$,

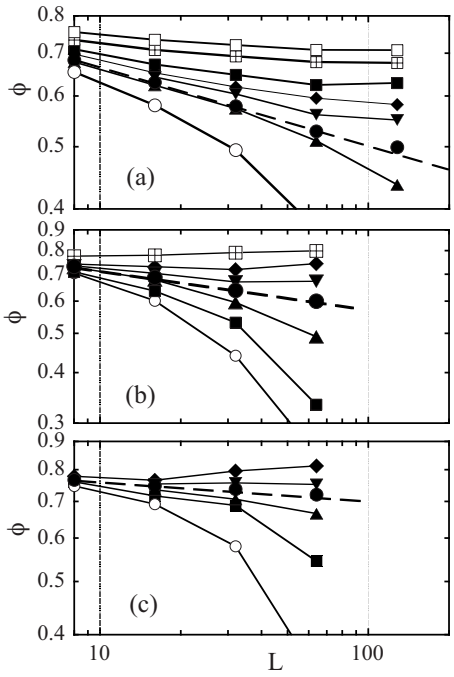


FIG. 4. Log-log plots of $\phi$ vs system size $L$, for SCD's with $h_4=0$, at (□) $T=0.52$, (⊞) $T=0.54$, (■) $T=0.56$, (♦) $T=0.57$, (▼) $T=0.575$, (●) $T=0.58$, (▲) $T=0.583$, and (○) $T=0.60$. Lines are only guides for the eyes, except for the dashed line, which stands for $\phi \sim L^{-\beta/\nu}$ with $\beta/\nu=0.13(2)$. (b) Same as in (a) but for SCD's with $h_4=4$ and (⊞) $T=0.84$, (♦) $T=0.85$, (▼) $T=0.855$, (●) $T=0.857$, (▲) $T=0.860$, (■) $T=0.865$, (○) $T=0.87$. Lines are only guides to the eye, except for the dashed line, which stands for $\phi \sim L^{-\beta/\nu}$ with $\beta/\nu=0.10$. (c) Same as in (a) but for $h_4=\infty$, with (♦) $T=1.10$, (▼) $T=1.103$, (●) $T=1.105$, (▲) $T=1.107$, (■) $T=1.110$, and (○) $T=1.115$. Lines are only guides for the eyes, except for the dashed line, which stands for $\phi \sim L^{-\beta/\nu}$ with $\beta/\nu=0.04(2)$.

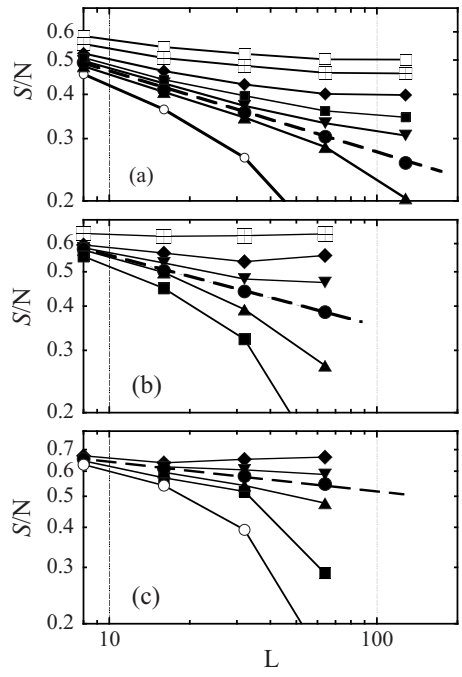


FIG. 5. (a) Log-log plots of $\mathcal{S}/N$ vs system length $L$, for SCD's with $h_4=0$, at (□) $T=0.52$, (⊞) $T=0.54$, (♦) $T=0.56$, (■) $T=0.57$, (▼) $T=0.575$, (●) is for $T=0.58$, and (▲) is for $T=0.583$, and (○) $T=0.60$. The dashed line stands for $\mathcal{S}/N \sim L^{-\eta}$, with $\eta=0.23$. Other lines are only guides for the eyes. (b) Same as in (a) but for SCD's with $h_4=4$ at (⊞) $T=0.84$, (♦) $T=0.85$, (▼) $T=0.855$, (●) $T=0.857$, (▲) $T=0.860$, (■) $T=0.865$. The dashed line stands for $\mathcal{S}/N \sim L^{-\eta}$ with $\eta=0.19(2)$. Other lines are only guides for the eyes. (c) Same as in (a) but for $h_4=\infty$, with (♦) $T=1.10$, (▼) $T=1.103$, (●) $T=1.105$, (▲) $T=1.107$, (■) $T=1.11$, and (○) $T=1.115$. The dashed line is for $L^{-\eta}$, where $\eta=0.10$. Other lines are only guides to the eye.

where $f_2(x)$ and $f_3(x)$ are some functions of $x$.

We first determine the values of $T_c$, making use of the fact that $f_1$, $f_2$ and $f_3$ do not depend on $L$ at $T=T_c$. We therefore look for straight line behavior in Figs. 4(a), 4(b), and 4(c), Figs. 5(a), 5(b), and 5(c), and Figs. 6(a)–6(c). We thus arrive at the values of $T_c$ shown in Table I for $h_4=0$, 4, and $\infty$. The errors in $T_c$ and the ensuing errors in the critical indices are discussed at the end of this section.

The values of $T_c$ in Table I are next used for the determination of the critical indices. Consider Fig. 4(a). The straight dashed line therein stands for $\phi \propto L^{-\beta/\nu}$, with $\beta/\nu=0.13$. From the error in $T_c$, we estimate an error of 0.02 for $\beta/\nu$. Analogously, we obtain the values and errors of $\beta/\nu$ for $h_4=4$ and $\infty$ from the plots in Figs. 4(b) and 4(c). The values of $\eta$ are obtained similarly from the plots in Figs. 5(a), 5(b), and 5(c). For $\alpha/\nu$, we first examine Fig. 6(a). A straight line seems to hold only at $T=0.58$ for $32<L$. Extrapolation of this straight line would give $\alpha/\nu \simeq 0.1$. However, this result does not seem to be on firm ground. The straight line would no longer look to be so if, for instance, we shift a single data point, the one for $L=128$, downward by 2%. This is 2 times the size of the error. On the other hand, we can safely draw the conclusion, from the data points shown in Fig. 6(a), that $\alpha/\nu \lesssim 0.1$ for $h_4=0$. We obtain $\alpha/\nu$ for $h_4=4$ and $h_4=\infty$ from the plots in Figs. 6(b) and 6(c). The values thus obtained for $\beta/\nu$, $\eta$, and $\alpha/\nu$ are listed in Table I.

In order to obtain the value of $\nu$, defined by $\xi \sim |T-T_c|^{-\nu}$, we note that scaling, more specifically, Eq. (9), implies that plots of $\phi L^{\beta/\nu}$ vs $L|T-T_c|^{\nu}$ for different values of $L$ fall into the same curve if the right values of $T_c$, $\beta/\nu$, and $\nu$ are used. Such plots are shown in Fig. 7(a) for $h_4=0$, using $T_c=0.580$, $\beta/\nu=0.13$, and $\nu=1.05$. Worse fits are obtained for $\nu=1.0$ or $\nu=1.1$. This is the basis for the value $\nu=1.05(5)$ shown in Table I. We proceed similarly for $h_4=4$ and $h_4=\infty$, making use of the plots shown in Figs. 7(b) and 7(c), respectively. We thus obtain $\nu=0.70(5)$ and $\nu=0.67(5)$ for $h_4=4$ and $h_4=\infty$, respectively. We have performed scaling plots (not shown) for other physical variables as well. Specific heat scaling plots yield slightly different values of $\nu$: 0.77(5) and 0.72(5) for $h_4=4$ and $h_4=\infty$, respectively. These numbers differ slightly from the ones obtained from scaling $\phi$ vs $T$, but fall within the given errors. We list values of $\nu$ in Table I which are averages over numbers so obtained. We find no scaling for $h_4=0$, that is, plots for different values of $L$ do not collapse onto one single curve, which is as expected for $\alpha<0$.

Finally, the errors in the critical indices follow from errors in $T_c$, and from errors in the values of $\phi$, $\mathcal{S}$, and $C$. However,

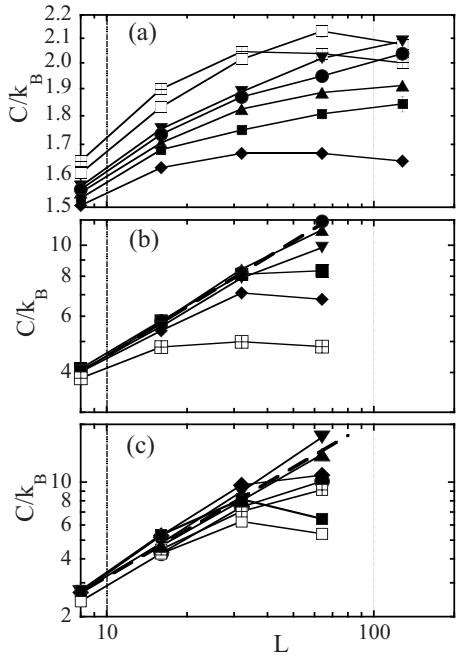


FIG. 6. (a) Log-log plots of the specific heat vs system length $L$, for SCD's with $h_4=0$, at (○) $T=0.54$, (♦) $T=0.56$, (■) $T=0.57$, (⊞) $T=0.575$, (▲) $T=0.58$ (▼) $T=0.583$, (□) $T=0.60$, (●) $T=0.62$. No straight line seems to fit the data points for any temperature, which suggests that $\alpha \lesssim 0$. (b) Same as in (a) but for SCD's with $h_4=4$, at (⊞) $T=0.84$, (♦) $T=0.85$, (▼) $T=0.855$, (●) $T=0.857$, (▲) $T=0.860$, (■) $T=0.865$. The dashed line is for $C/k_B \sim L^{\alpha/\nu}$ and $\alpha/\nu=0.51$. (c) Same as in (a) but for $h_4=\infty$, at (□) $T=1.10$, (⊞) at $T=1.103$, (●) $T=1.105$, (▲) $T=1.107$, (▼) $T=1.11$, (♦) $T=1.115$, and (■) at $T=1.12$. The dashed line is for $C/k_B \propto L^{0.9}$. Lines are only guides for the eyes.

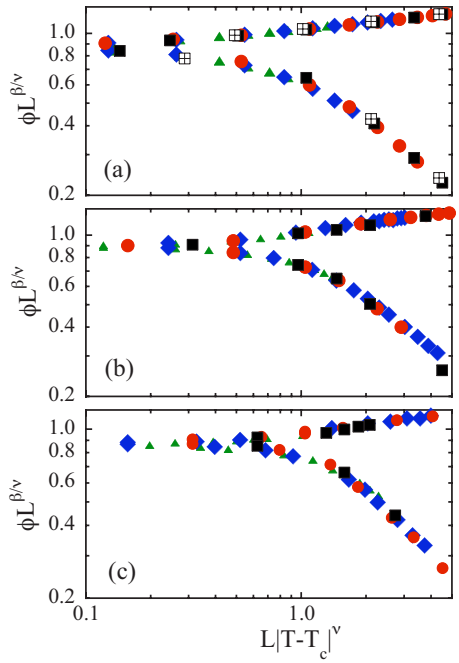


FIG. 7. (Color online) (a) Log-log plot of $\phi L^{\beta/\nu}$ vs $L|T-T_c|^{\nu}$, for SCD's with $h_4=0$, for $\beta/\nu=0.13$, $\nu=1.05$, and $T_c=0.580$. ▼, ♦, ●, ■, and ⊞ stand for $L=8,16,32,64$, and $L=128$, respectively. (b) Same as in (a) but only for $L \leq 64$, for SCD's with $h_4=4$, for $\beta/\nu=0.10$, $\nu=0.70$, and $T_c=0.8575$. ▲, ♦, ●, and ■ stand for $L=8,16,32$, and 64, respectively. (c) Same as in (b) but for $h_4=\infty$, with $\beta/\nu=0.06$, $\nu=0.67$, and $T_c=1.106$.

errors in the latter quantities are no larger than the symbol's sizes in any one of the figures, and are therefore less important than errors in $T_c$. Systems of $L \gtrsim 256$ would have to be simulated in order to reduce the latter errors. We have not done so because a MC run of $10^7$ MC sweeps on a system $256 \times 256$ spins with dipole-dipole interactions would require nearly one year of time of a single processor running at some 3 MHz.

## IV. SUMMARY

We next summarize the main results we have obtained for the thermal order-disorder phase transition of SCD's on a square lattice, for $h_4=0$, 4, and $\infty$. Let us first recall that even when $h_4=0$, SCD's in 2D have a residual quadrupolar anisotropy at nonzero temperatures,[9–11] coming from dipole-dipole interactions. Near the critical point, this residual anisotropy is approximately as if $h_4 \approx 0.5$, as can be gathered from Fig. 6 in Ref. 6. Effects coming from this residual anisotropy are illustrated in Fig. 1(d).

Our numerical results are consistent with a single thermal transition between the paramagnetic and antiferromagnetic phases. For $h_4=0$, this is not as immediately obvious as for $h_4=4$ and $\infty$. For $h_4=0$, we find below $T_c$ [see Fig. 4(a)] a small-to-large scale crossover which is consistent (a) with weak algebraic decay of the spin-spin correlation functions for short distances ($r \lesssim 100$) and (b) strong long-range order for longer distances. A single transition between the paramagnetic and the fully ordered phase is also what José *et al.*[17] found for the anisotropic $XY$ model, but is in contrast to the results of Rastelli *et al.*,[20] who inferred, from MC simulations, the existence of an intermediate phase between the paramagnetic and the fully ordered phase for $0 \lesssim h_4 \lesssim 0.5|J|$, where $J$ is the exchange constant. However, since the thermally induced anisotropy in SCD's in square lattices is as if $h_4 \approx 0.5$,[6] an intermediate phase in the $-0.5 \lesssim h_4 \lesssim 0$ may still be found in SCD's on square lattices.

Radically different critical behavior from the isotropic $XY$ model is expected for SCD's with $h_4=0$, because of the residual quadrupolar anisotropy that is induced at nonzero temperatures by dipole-dipole interactions. Indeed, we then find, within errors, a 2D Ising-type critical behavior. This is as conjectured by Prakash and Henley,[10] but differs from the MC results of Ref. 23 and from the renormalization group prediction of Ref. 16.

We also find that the critical behavior of SCD's on square lattices is nonuniversal, that critical index values (see Table I) vary with $h_4$, as they do in the anisotropic $XY$ model.[17,24] The variation of the specific heat's critical index, $\alpha$, is the most obvious one. However, the analogy with the ordinary $XY$ model is not very close. The difference is most easily appreciated for $h_4=\infty$. For SCD's with $h_4=\infty$, that is, for the D4CM, both the order parameter and the energy change rather abruptly at the critical point, more precisely, rather

large (small) $\alpha$ ($\beta$) index values are found (see Table I). This differs markedly from the behavior of the ordinary four-state clock model in 2D, which has long been known[25] to decouple into two independent 2D Ising models.

**ACKNOWLEDGMENTS**

Financial support from Grant No. FIS2006-00708, from the Dirección General de Investigación del Ministerio de Educación y Ciencia of Spain, is gratefully acknowledged.

*Electronic address: jefe@unizar.es; URL: http://Pipe.Unizar.Es/~jff

†Electronic address: jjalonso@darnitsa.cie.uma.es

[1] R. P. Cowburn, Philos. Trans. R. Soc. London, Ser. A **358**, 281 (2000); R. J. Hicken, *ibid.* **361**, 2827 (2003).

[2] R. F. Wang, C. Nisoli, R. S. Freitas, J. Li, W. McConville, B. J. Cooley, M. S. Lund, N. Samarth, C. Leighton, V. H. Crespi, and P. Schiffer, Nature (London) **439**, 303 (2006).

[3] See, for instance, D. Gatteschi and R. Sessoli, in *Magnetism: Molecules to Materials*, edited by J. S. Miller and M. Drillon (Wiley-VCH, Weinheim, 2002), Vol. III, Chap. 3; E. M. Chudnovsky and J. Tejada, *Macroscopic Quantum Tunneling of the Magnetic Moment* (Cambridge University Press, Cambridge, 1998); D. Gatteschi, R. Sessoli, and J. Villain, *Molecular Nanomagnets* (Oxford University Press, Oxford, 2006).

[4] J. F. Fernández and J. J. Alonso, Phys. Rev. B **62**, 53 (2000).

[5] R. Siddharthan, B. S. Shastry, A. P. Ramirez, A. Hayashi, R. J. Cava, and S. Rosenkranz, Phys. Rev. Lett. **83**, 1854 (1999); A. P. Ramirez, A. Hayashi, A. Cava, R. J. Siddharthan, and B. S. Shastry, Nature (London) **399**, 333 (1999); S. T. Bramwell and M. J. P. Gingras, Science **294**, 1495 (2001).

[6] J. J. Alonso and J. F. Fernández, Phys. Rev. B **74**, 184416 (2006).

[7] P. I. Belobrov, R. S. Gekht, and V. A. Ignatchenko, Zh. Eksp. Teor. Fiz. **84**, 1097 (1983); [Sov. Phys. JETP **57**, 636 (1983)].

[8] J. F. Fernández and J. J. Alonso, Phys. Rev. B **73**, 024412 (2006).

[9] K. De'Bell, A. B. MacIsaac, I. N. Booth, and J. P. Whitehead, Phys. Rev. B **55**, 15108 (1997).

[10] S. Prakash and C. L. Henley, Phys. Rev. B **42**, 6574 (1990).

[11] E. Rastelli, S. Regina, A. Tassi, and A. Carbognani, Phys. Rev. B **65**, 094412 (2002).

[12] N. D. Mermin and H. Wagner, Phys. Rev. Lett. **17**, 1133 (1966).

[13] S. Romano, Phys. Rev. B **44**, 7066 (1991).

[14] By weak long-range order we mean, as is usual, that spin-spin correlations decay algebraically, with distance.

[15] S. V. Maleev, Zh. Eksp. Teor. Fiz. **70**, 2375 (1976); [Sov. Phys. JETP **43**, 1240 (1976)].

[16] P. G. Maier and F. Schwabl, Phys. Rev. B **70**, 134430 (2004).

[17] J. V. José, L. P. Kadanoff, S. Kirkpatrick, and D. R. Nelson, Phys. Rev. B **16**, 1217 (1977); see also F. Y. Wu, Rev. Mod. Phys. **54**, 235 (1982).

[18] N. A. Metropolis, A. W. Rosenbluth, M. N. Rosenbluth, A. H. Teller, and E. Teller, J. Chem. Phys. **21**, 1087 (1953).

[19] See, for instance, M. S. S. Challa and D. P. Landau, Phys. Rev. B **33**, 437 (1986).

[20] E. Rastelli, S. Regina, and A. Tassi, Phys. Rev. B **70**, 174447 (2004).

[21] M. P. Nightingale and H. W. J. Blotte, Physica A **104**, 352 (1980); M. P. Nightingale and A. H. Hooft, Physica (Amsterdam) **77**, 390 (1974); V. Privman and M. E. Fisher, Phys. Rev. B **30**, 322 (1984).

[22] M. E. Fisher, Rev. Mod. Phys. **70**, 653 (1998).

[23] A. Carbognani, E. Rastelli, S. Regina, and A. Tassi, Phys. Rev. B **62**, 1015 (2000).

[24] E. Rastelli, S. Regina, and A. Tassi, Phys. Rev. B **69**, 174407 (2004).

[25] M. Suzuki, Prog. Theor. Phys. **13**, 770 (1967).